Reaction Chemistry & Engineering

ROYAL SOCIETY OF CHEMISTRY

COMMUNICATION

View Article Online
View Journal | View Issue

Cite this: *React. Chem. Eng.*, 2025, **10**, 2238

Received 29th May 2025,
Accepted 17th August 2025

DOI: 10.1039/d5re00239g

rsc.li/reaction-engineering

Short reaction times for hydrogenolysis of polyolefins by overcoming mass transfer limitations

E. van Daatselaar, [a] A. G. J. van der Ham,[a] S. R. A. Kersten[a] and M. P. Ruiz *[ab]

The recycling of polyolefins is gaining attention as society transitions toward a more circular economy. Pyrolysis is a promising method; however, its product distribution can be unpredictable. Moreover, the resulting compounds often require additional hydrogenation if they are to be used as feedstock for naphtha crackers. An alternative approach is hydrogenolysis, in which polyolefins are depolymerised into shorter, fully saturated alkanes using a heterogeneous catalyst under a hydrogen atmosphere. Literature indicates that the hydrogenolysis of polyolefins appears to be a slow process, requiring reaction times up to 96 hours to achieve a significant yield of useful products, such as naphtha or fuels. In this work, it is shown that these long reaction times are resolved when physical mass transport limitations are overcome: in 40 minutes, full conversion of low-density polyethylene to gas and liquid products is reached. Introducing a hollow-shaft mechanical stirrer instead of no or limited stirring significantly increases the gas contact area and mass transfer coefficient to the polymer melt, resulting in a decrease in mass transport limitations and thus an increase in overall reactivity. Monitoring the (hydrogen) pressure over time generates more insight into the reaction kinetics, as at a similar hydrogen consumption level, the product distribution changes if the system is stirred instead of kept stagnant. The authors would like to emphasise the importance of these findings regarding the influence of hydrogen mass transfer through the melt, as this could also result in novel catalysts possibly performing even better than currently reported, making hydrogenolysis a more viable option for the chemical recycling of polyolefins.

In recent years, an increasing number of scientific articles have been published researching the application of hydrogenolysis as a novel chemical recycling technique for the conversion of polyolefins, such as polyethylene and polypropylene, to smaller alkanes used as fuels or as feedstock for the existing plastic production process.[1–9] Published work focuses mainly on the development of highly active catalysts and the research on reaction mechanisms, to be able to obtain full conversion and, preferably, high yields in the liquid and wax range. This mixture with compounds in the range of pentane (C_5H_{12}) to eicosane ($C_{20}H_{42}$), is the desired product, as the lower range is similar to the naphtha feedstock for hydrocrackers, while the higher range equals fuel in the gasoline or diesel range. However, current reported reaction times to reach this product distribution are substantial, ranging from 3 to 96 hours.[2,3,7,10] Reaction times must be significantly reduced to develop an economically feasible chemical recycling process of polyolefin waste into fuels using hydrogenolysis.

Current literature often neglects the influence of, amongst others, feedstock, and reactor kinetics and configuration.[11–13] As the scission of the polyolefins depends on the presence of hydrogen at the catalyst surface in the liquid phase,[10] we prove in this work that mass transfer of hydrogen is of high importance to be able to quickly hydrogenolyse polyolefins.

In published work, hydrogenolysis of polyolefins is often performed with a monofunctional ruthenium on carbon (Ru/C) catalyst, either as the main focus or as a benchmark experiment. In Table 1, an overview of several studies that apply similar reaction conditions, such as temperature and initial hydrogen pressure, is given. The reactor volumes are comparable, ranging from 25 to 190 mL.[2,5] The main difference is the level of stirring: either not at all, with a magnetic bar, or a mechanical impeller. As can be seen in Table 1, to achieve full conversion of the polymer to gases and liquids using Ru/C, reaction times of up to 24 hours are required. To enable a consistent comparison of the literature data, the required hydrogen consumption in moles was calculated from the reported product distributions, extracted from either figures or tables. Complete saturation of all products was assumed. Per mole of converted polyolefin, this corresponds to a hydrogen usage of $x - 1$ moles of H_2, where

[a] *Sustainable Process Technology, University of Twente, PO Box 217, 7500 AE Enschede, The Netherlands. E-mail: m.p.ruizramiro@utwente.nl*
[b] *Circular Chemical Engineering, Maastricht University, 6167 RD Geleen, The Netherlands*

Table 1 Overview of publications performing hydrogenolysis of polyolefins over a monofunctional ruthenium catalyst. The hydrogen consumption rates are calculated based on reported data, assumptions can be found in section S1

Feed (MW)	Catalyst[a]	Type of stirring	Stirring rate [rpm]	Ratio F : C	Mass feed [g]	Temp. [°C]	Initial H_2 press. (STP) [bar]	Reaction time [h]	Gas yield (C1–C4) [wt%]	Liquid yield (C5–C45) [wt%]	Solid yield (C45+) [wt%]	H_2 cons. rate (calc. & norm.) [$mol_{H_2}\ g_{Ru}^{-1}\ s^{-1}$]	Source
LDPE (4 kDa)	Ru/C	No stirring	—	10 : 1	1.0	250	30	18	100	0	0	1.9×10^{-4}	1
LDPE (4 kDa)	Ru/C	Magnetic	600	25 : 1	1.4	200	22	16	57	43	0	2.8×10^{-4}	2
LDPE (4 kDa)	Ru/C	Magnetic	600	4 : 1	0.1	225	30	16	100	0	0	7.6×10^{-5}	2
i-PP (250 kDa)	Ru/C	Magnetic, 0.7 mL stir bar	300	20 : 1	2.0	250	30	16	97	3	0	3.8×10^{-4}	3
LDPE (~100 kDa)	Ru/CeO_2[b]	Magnetic	400	4 : 1	2.0	250	20	24	13	87	0	3.0×10^{-4}	4
LDPE (4 kDa)	Ru/C	Magnetic, glass coated stir bar	450	34 : 1	3.4	240	35	6	23	39	38	2.7×10^{-4}	5
HDPE (200 kDa)	Ru/TiO_2	Mechanical, solid shaft	750	20 : 1	0.5	225	20	4	60[c]	14[c]	26	4.8×10^{-4}[d]	6
LDPE (4 kDa)	Ru/C	Mechanical, hollow shaft	1300	9.3 : 1	3.5	250	40	0.67	22	78	0	1.4×10^{-3}	This work

[a] 5 wt% Ru, unless noted otherwise. [b] 0.2 wt% Ru. [c] Gas range reported as sum of C1–C5, liquid range starts at C6. [d] Based on reported reaction rate.

$x - 1$ equals the total number of moles of alkane products formed. This approach ensures closure of both the carbon and hydrogen balances. The required amount of moles H_2 to obtain the given product distributions is normalised over the amount of ruthenium and averaged over the reaction time ($mol_{H_2}\ g_{Ru}^{-1}\ s^{-1}$). The assumptions for these calculations can be found in the SI, section S1.

This work reevaluates the same reaction system of LDPE (MW 4 kDa) and 5 wt% Ru/C, while applying a novel reactor configuration. As hydrogen is required to hydrogenolyse the polyolefins, a higher concentration of hydrogen in the polymer melt near the catalyst surface should enhance the reaction rate. For that reason, a hollow shaft stirrer is applied, which physically introduces hydrogen bubbles in the liquid phase, increasing the contact area and thus the mass transfer of hydrogen from the gas phase to the liquid phase (Fig. 1 and S5). During operation of this batch-wise system, the pressure and temperature are logged over the entire reaction time, resulting in information about the reactivity of the chemical system. More details on the experimental method, reactor set-up and components, all designed and built in-house, can be found in the SI (section S2).

As the reaction progresses, the measured pressure in the reactor is a combination of the hydrogen and product partial pressures in the gas phase, *i.e.* $P_{tot} = P_{H_2,G} + P_{C_x,G}$. A pressure change is thus a direct result of both consumption of H_2 and the formation of gaseous hydrocarbons (C_x). The concentration of H_2 in the liquid is proportional to the concentration (and thus partial pressure) of hydrogen in the gas phase *via* the solubility ($C_{H_2,L} = m \times C_{H_2,G}$), the volumetric mass transfer coefficient k_La and consumption during reaction. Due to the mixing shown in Fig. 1 and S5, the value for k_La is high. Measurements and calculations in section S3

Fig. 1 Schematic overview of the hollow-shaft stirred autoclave. Due to rotation, hydrogen gas is transported through the shaft into the polymer melt, increasing the gas transport area through bubble formation.

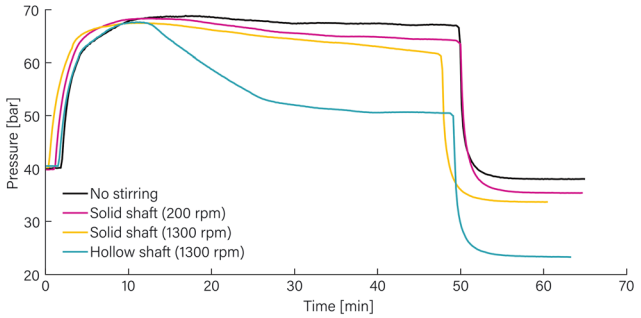

Fig. 2 Pressure over time for experiments undergoing different stirring regimes, including heating and cooling time. Experimental settings: 3.5 g LDPE, Ru/C, feed-to-catalyst 9.3 to 1, 40 bar H_2 (at RT), initial peak temperature 260 ± 5 °C, after 15 min 250 ± 5 °C. At $t \approx 50$ min: end of experiment and fast cooling of contents.

return a k_La of 0.114 s^{-1}, which is in line with literature.[14] The calculated mass transfer rate is approximately six times higher than the experimentally measured consumption rate, indicating that observing the intrinsic chemical kinetic rate of the reaction is being approached. Moreover, in section S3, it is also shown that the reaction rate has a first-order dependence on the catalyst amount.

Performing batch reactions with LDPE (4 kDa) and 5 wt% Ru/C at a feed-to-catalyst ratio 9.3 to 1, 250 °C and an initial pressure 40 bar H_2 (at RT) for 40 minutes at reaction temperature, while changing the stirring regime, returns pressure profiles as shown in Fig. 2. This raw data shows a difference in reaction rate, as no stirring results in nearly no pressure decrease and thus almost no polymer conversion. Stirring with a solid shaft at different speeds to mimic recent work using magnetic or mechanical stirrers does increase the conversion rate minimally, as the slope steepens slightly. However, applying the hollow shaft stirrer shows a significant pressure drop, indicating much more conversion within the same time range.

To determine an actual value for the hydrogen consumption rate to compare with existing literature data, the raw pressure data is fitted, as well as the final hydrogen partial pressure at operating temperature ($P_{H_2,G} = y_{H_2} \times P_{tot}$). The volume fraction y_{H_2} is measured with GC and P_{tot} is the final pressure before cooling down. The slopes of these fits give respectively the total molar change and the hydrogen consumption over time and are shown in Fig. 3 for the hollow-shaft stirred experiment. Normalising these obtained values for the amount of ruthenium in the catalyst results in the desired rates. Following these calculations, the hydrogen consumption rate for a system stirred with this hollow shaft stirrer is 1.4×10^{-3} mol_{H_2} g_{Ru}^{-1} s^{-1}. Applying the method discussed before, *i.e.*, calculating the required amount of H_2 by setting $x - 1$ equal to the amount of moles formed product (section S1), to the same experimental data results in a similar value (±7%), showing that both the method requiring the fit and the method used for the analysis of the literature data are interchangeable. This makes the comparison of obtained values in this work with the literature data in Table 1 valid.

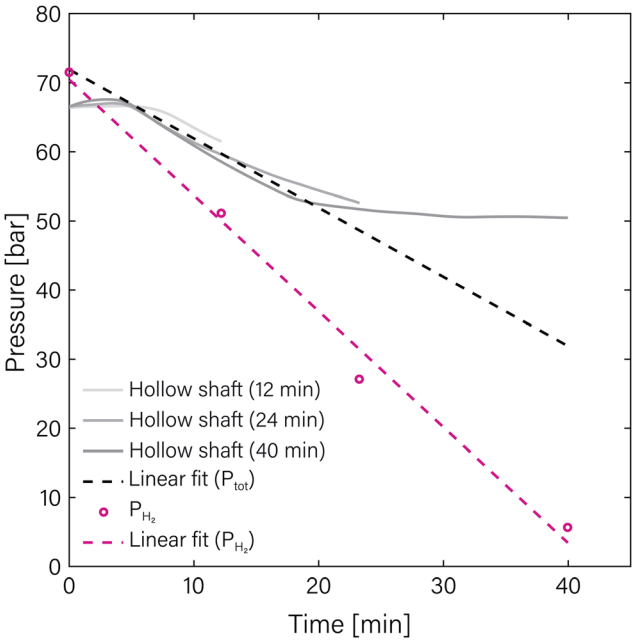

Fig. 3 Pressure over time for hollow-shaft stirred experiments for different reaction times (grey). Pink dots indicate final partial hydrogen pressure. Linear fits are shown (dashed) to extract rates. Experimental settings: 3.5 g LDPE, Ru/C, feed-to-catalyst 9.3 to 1, 40 bar H_2 (at RT), initial peak temperature 260 ± 5 °C, after 15 min 250 ± 5 °C.

Calculating the rates for the experiments with no or limited stirring results in similar values for the normalised hydrogen consumption compared to data shown in Table 1,[1,5,6] namely 1.48×10^{-4} and 2.78×10^{-4} mol_{H_2} g_{Ru}^{-1} s^{-1}, respectively. These calculations can be found in the SI, section S4. More importantly, compared to the performed non-stirred experiment, the consumption rate of the hollow-shaft stirred system is approximately 10 times faster (Table S5), *i.e.* this finding significantly reduces the required reaction times to obtain liquid yields *via* hydrogenolysis. Analysis of the final product substantiates this statement, as the product is fully converted to alkanes in the range of C1 to C28 within the reaction time of 40 minutes – see Fig. 5.

As previously mentioned, the measured pressure is a combination of hydrogen consumption and gaseous product formation. Therefore, the resulting product distribution was expected to resemble when experiments reach a comparable final pressure. The pressure profiles of a non-stirred and hollow-shaft stirred experiment, conducted for 420 and 24 minutes, respectively, are presented in Fig. 4 together with the earlier shown 40 minute experiment for comparison. An identical final reactor pressure is reached within a ±0.5% margin. However, comparing the resulting product yields in Fig. 5 reveals unexpected results: the enhanced mass transfer influences the product distribution.

As can be seen in Fig. 5, not stirring the reaction mixture does lead to the formation of lower molecular weight alkanes. The methane yield of 15 wt% is notably higher compared to the methane yield of the hollow-shaft stirred reaction mixtures, while the formation of other gases remains

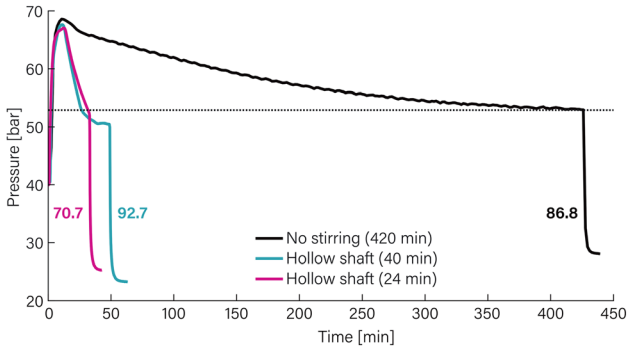

Fig. 4 Pressure over time for a non-stirred (420 min) and hollow-shaft stirred (24 min, 1300 rpm) experiment, reaching both a final pressure of 52.7 (±0.5%) bar, dashed line to guide the eye. Hollow-shaft stirred (40 min, 1300 rpm) experiment for comparison. Heating and cooling time is included. Bold values represent the total consumption of hydrogen per experiment in wt%, measured by GC analysis. Experimental settings: 3.5 g LDPE, Ru/C, feed-to-catalyst 9.3 to 1, 40 bar H_2 (at RT), initial peak temperature 260 ± 5 °C, after 15 min 250 ± 5 °C. At end of experiment: fast cooling of contents.

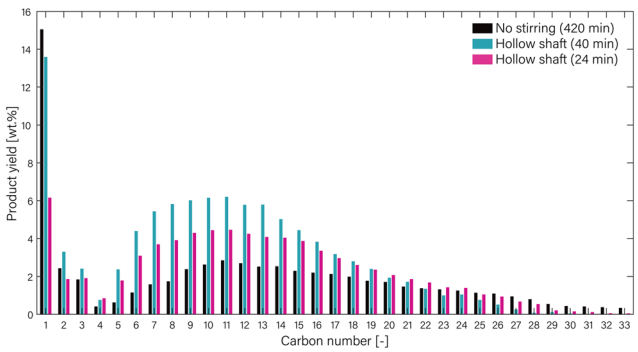

Fig. 5 Product distribution in the liquid range for non-stirred (420 min) and hollow shaft-stirred (40 and 24 min, both 1300 rpm) experiments. Significant dip in butane (C_4H_{10}) is due to a limited range for gas analysis and handling. Approximately 1 wt% is missing. Experimental settings: 3.5 g LDPE, Ru/C, feed-to-catalyst 9.3 to 1, 250 °C, 40 bar H_2 (at RT).

in the same order of magnitude. This suggests a higher occurrence of end-chain scissions when not stirred. After 24 minutes of reaction time in the stirred experiments, only 6 wt% of methane has formed. Also at this point, a significant amount of liquid alkanes has already formed. Comparing to the 40 minute experiment, it seems that these alkanes are partly converted to methane and other lighter alkanes, increasing the partial pressure of hydrocarbons $P_{C_x,G}$, resulting in the change of slope in Fig. 4. Additionally, the liquid formation due to the rapid conversion in the stirred reactor also leads to a drop in viscosity, as can already be seen in the physical products (Fig. S11). Distributing the hydrogen gas, catalyst, and remaining polymers will be faster, even as dissolving hydrogen. The fractional molar solubility of hydrogen, *i.e.*, mol_{H_2} per mol alkane, decreases in lower alkanes;[15,16] however, the number of moles present in the melt increases nearly exponentially due to the alkane scission, leading to an increase in the absolute amount of dissolved hydrogen moles per volume. Both these phenomena will result in an enhanced reaction rate to either liquid or gaseous products. This explains the sudden increase in methane formation from 24 to 40 minutes. Combining this data, it is hypothesised that the increased concentration of H_2 in the melt or liquid phase – and thus at the catalyst surface – due to stirring with a hollow shaft stirrer, alters the ratio of end and random chain scission, favouring the latter and hence promoting the formation of liquids. More specifically, the cleavage of primary–secondary carbon bonds will keep happening, but the occurrence of secondary–secondary carbon bond scission is increased.

These findings have a considerable impact on existing data in catalyst research. As it is often not reported if or how well the reaction systems are stirred, the mass transfer limitations of hydrogen to the catalyst surface could have inhibited the observed reaction rates and influenced the obtained product distribution. To ensure meaningful comparisons between catalysts, it is critical that researchers assess the extent of mass transfer limitations in their systems before drawing conclusions about the activity and reactivity of catalysts applied in hydrogenolysis.

Author contributions

EvD performed all experiments and wrote the manuscript. AGJvdH, SRAK and MPR acquired funding, gave guidance and research direction, reviewed the results and manuscript.

Conflicts of interest

There are no conflicts to declare.

Data availability

Supplementary information available: The supplementary information includes a detailed description of the experimental set-up and methods, as well as the mass balance closure data of the experiments, and the procedure followed for the calculations of the hydrogen consumption rate. See DOI: **https://doi.org/10.1039/D5RE00239G**.

The data supporting this article have been included as part of the SI.

Acknowledgements

The authors would like to thank Ronald Borst, Benno Knaken, Raymond Spanjer and Erna Fränzel-Luiten for their technical support in this work.

References

1 L. Chen, Y. Zhu, L. C. Meyer, L. V. Hale, T. T. Le, A. Karkamkar, J. A. Lercher, O. Y. Gutierrez and J. Szanyi, *React. Chem. Eng.*, 2022, **7**, 844–854.
2 J. E. Rorrer, G. T. Beckham and Y. Roman-Leshkov, *JACS Au*, 2021, **1**, 8–12.

3 P. A. Kots, S. Liu, B. C. Vance, C. Wang, J. D. Sheehan and D. G. Vlachos, *ACS Catal.*, 2021, **11**, 8104–8115.
4 M. Chu, X. Wang, X. Wang, X. Lou, C. Zhang, M. Cao, L. Wang, Y. Li, S. Liu, T.-K. Sham, Q. Zhang and J. Chen, *Research*, 2023, **6**, 1–10.
5 Y. Nakaji, M. Tamura, S. Miyaoka, S. Kumagai, M. Tanji, Y. Nakagawa, T. Yoshioka and K. Tomishige, *Appl. Catal., B*, 2021, **285**, 119805.
6 S. D. Jaydev, A. J. Martin, D. Garcia, K. Chikri and J. Perez-Ramirez, *Nat. Chem. Eng.*, 2024, **1**, 565–575.
7 G. Celik, R. M. Kennedy, R. A. Hackler, M. Ferrandon, A. Tennakoon, S. Patnaik, A. M. LaPointe, S. C. Ammal, A. Heyden, F. A. Perras, M. Pruski, S. L. Scott, K. R. Poeppelmeier, A. D. Sadow and M. Delferro, *ACS Cent. Sci.*, 2019, **5**, 1795–1803.
8 S. D. Jaydev, A. J. Martin and J. Perez-Ramirez, *ChemSusChem*, 2021, 1–8.
9 Z. Qiu, S. Lin, Z. Chen, A. Chen, Y. Zhou, X. Cao, Y. Wang and B. L. Lin, *Sci. Adv.*, 2023, **9**, 1–10.
10 Y. Nakagawa, S. I. Oya, D. Kanno, Y. Nakaji, M. Tamura and K. Tomishige, *ChemSusChem*, 2017, **10**, 189–198.
11 P. A. Kots, B. C. Vance and D. G. Vlachos, *React. Chem. Eng.*, 2022, **7**, 41–54.
12 R. Helmer and M. Shetty, *Chem Catal.*, 2023, **3**, 1–2.
13 M. L. Pennel, Y. Jiang and M. Cargnello, *ACS Sustainable Resour. Manage.*, 2024, **1**, 1047–1052.
14 A. Buffo, M. Vanni and D. Marchisio, *Chem. Eng. Sci.*, 2012, **70**, 31–44.
15 M. N. Amar, F. M. Alqahtani, H. Djema, K. Ourabah and M. Ghasemi, *J. Taiwan Inst. Chem. Eng.*, 2023, **153**, 105215.
16 M.-R. Mohammadi, F. Hadavimoghaddam, M. Pourmahdi, S. Atashrouz, M. T. Munir, A. Hemmati-Sarapardeh, A. H. Mosavi and A. Mohaddespour, *Sci. Rep.*, 2021, **11**, 17911.

